Modulational instability of charge transport in the Peyrard–Bishop–Holstein model

2009 J. Phys.: Condens. Matter 21 335101

(http://iopscience.iop.org/0953-8984/21/33/335101)

J. Phys.: Condens. Matter **21** (2009) 335101 (7pp) doi:10.1088/0953-8984/21/33/335101

Modulational instability of charge transport in the Peyrard–Bishop–Holstein model

Conrad Bertrand Tabi[1,2], Alidou Mohamadou[1,3] and Timoléon Crépin Kofané[1]

[1] Laboratory of Mechanics, Department of Physics, Faculty of Science, University of Yaounde I, PO Box 812, Yaounde, Cameroon
[2] The Abdus Salam International Center For Theoretical Physics, PO Box 586, Strada Costiera 11, I-34014 Trieste, Italy
[3] Condensed Matter Laboratory, Department of Physics, Faculty of Science, University of Douala, PO Box 24157, Douala, Cameroon

E-mail: contab408@hotmail.com, mohdoufr@yahoo.fr and tckofane@yahoo.com

Received 2 December 2008, in final form 10 June 2009
Published 8 July 2009
Online at stacks.iop.org/JPhysCM/21/335101

Abstract

We report on modulational instability (MI) on a DNA charge transfer model known as the Peyrard–Bishop–Holstein (PBH) model. In the continuum approximation, the system reduces to a modified Klein–Gordon–Schrödinger (mKGS) system through which linear stability analysis is performed. This model shows some possibilities for the MI region and the study is carried out for some values of the nearest-neighbor transfer integral. Numerical simulations are then performed, which confirm analytical predictions and give rise to localized structure formation. We show how the spreading of charge deeply depends on the value of the charge–lattice-vibrational coupling.

(Some figures in this article are in colour only in the electronic version)

1. Introduction

The way DNA conducts charge remains an intriguing phenomenon to physicists and biologists alike. A specific motivation for studying this problem is an experiment on charge transport along a DNA molecule. Each of the two DNA strands may be viewed as a chain, each site of which is one of the four bases: guanine (G), adenine (A), cytosine (C) and thymine (T), having different ionization potentials. Thus, if one moves an electron from the chain, the resulting hole feels the on-site potentials $V_G < V_A < V_C < V_T$. It was thus suggested many years ago that the overlapping π orbitals of the nucleotide bases form a common delocalized electron system in the whole DNA macromolecule and so a Bloch-type description of the electron states becomes possible [1–3]. There are the results of some recent measurements indicating that DNA behaves as a well-conducting one-dimensional molecular wire [4, 5]. In contrast, it was reported that DNA is insulating [6] and, for short oligomers built up from base pairs of the same type, semiconductivity was observed [7]. This qualitative discrepancy is also shared by theoretical findings so that it remains unclear whether charge migration is possible or not in DNA. As a consequence, a detailed understanding of the charge transport mechanism of DNA also remains unclear. In this framework, we aim at studying such a phenomenon through modulational instability (MI). MI, which results from the interplay between dispersion and nonlinearity, has been shown to be a precursor to soliton and bubble formation. In the framework of DNA dynamics, soliton formation through MI has been investigated [8], which shows the possibility of soliton and the bearing of localized structures. So, particular attention will be paid to the patterns of charge spreading in the lattice.

As widely known, different attempts to model the charge transport of DNA were based on transport via coherent tunneling [1], classical diffusion under the condition of temperature-driven fluctuations [9], incoherent phonon-assisted hopping [10, 11] and variable range hopping between localized states [12] and solitons [13]. Recently, a polaron model has been shown to provide promising results as

well [14–19], especially for explaining the temperature dependence of DNA conductance [14, 15, 18]. Moreover, an additional advantage of the polaron model in comparison to the popular models such as the tight-binding approach or the system of kinetic equations is that it includes the interaction of the migrating charge with the DNA lattice.

The Peyrard and Bishop (PB) model [20] concentrates on transversal openings of base pairs. It is one of the simplest models that investigates DNA at the scale of a base pair [20, 21]. The complex double-stranded molecule is described by postulating some simple effective interactions among the bases within a pair and along the strands. The model has been successfully applied to analyze experiments on the melting of short DNA chains [22]. Furthermore, it allows us to easily include the effect of heterogeneities [23] yielding a sharp staircase structure of the melting curve (number of open base pairs as a function of the temperature T) [24]. Beyond its original motivation to explain the denaturation, the PB model has an intrinsic theoretical interest as one of the simplest one-dimensional systems displaying a genuine phase transition [25, 26]. Against this background, we use the Peyrard–Bishop–Holstein (PBH) model [16, 18] to study charge transport, through MI, in the DNA molecule. In fact, the PBH model combines a quantum-mechanical treatment of charge motion with a classical treatment of the lattice distortion dynamics in a highly flexible DNA molecule. For the sake of simplicity, to perform the linear stability analysis, we reduce the PBH model to a modified Klein–Gordon–Schrödinger (mKGS) model and numerical experiments are performed in the original PBH model.

This paper is therefore organized as follows: in section 2, we present the model and we reduce it to its continuum approximation. Linear stability analysis is also performed in this part and predictions on localized structure formation are discussed. In section 3, we perform numerical experiments on MI and we show that the analytical predictions are satisfied. A particular attention is paid to the dependence of charge density on the charge-vibrational coupling constant. Section 4 is devoted to some concluding remarks.

2. The PBH model and linear stability analysis

2.1. Model

The PBH model, as already said, was introduced [18, 27] as a coupled charge–lattice model for carrier migration in the high flexible DNA molecule. In a polychain, each strand contains only one base type. The purine and pyrimidine bases are characterized by different ionization potentials ($\leqslant$0.1 eV [28]). Because they belong to opposite strands in the poly-DNA, the main mechanism of charge migration is longitudinal one-dimensional tunneling along a single strand containing purine bases. The application of the polaron model for the description of the charge transfer in the poly-DNA molecule is limited by temperature due to the dependence on structural disorder induced by the polaron on the thermal fluctuations [18]. The model we consider in this work is therefore free of the influence of temperature and structural disorder [18]. Consequently, in the semiclassical approximation [16, 29], the coupled system of nonlinear equations based on this model is

$$\mathrm{i}\hbar\frac{\mathrm{d}\psi_n}{\mathrm{d}t} = -V(\psi_{n+1}+\psi_{n-1}) + \chi y_n\psi_n \tag{1}$$

$$m\frac{\mathrm{d}^2y_n}{\mathrm{d}t^2} = -\frac{\mathrm{d}V_{\mathrm{M}}(y_n)}{\mathrm{d}y_n} - \frac{\mathrm{d}W(y_n, y_{n-1})}{\mathrm{d}y_n} - \frac{\mathrm{d}W(y_{n+1}, y_n)}{\mathrm{d}y_n} - \chi|\psi_n|^2 \tag{2}$$

where ψ_n is the probability amplitude for the charge on the nth site, V is the nearest-neighbor transfer integral between base pairs, χ is the charge-vibrational coupling constant, y_n is the amount by which the nth base pair is displaced from its equilibrium position, m is the base pair mass on the single site, $V_{\mathrm{M}}(y_n)$ is the on-site Morse potential, which describes interactions between hydrogen bonds in a pair and $W(y_n, y_{n-1})$ is the interaction of neighboring stacked base pairs. The expressions for V_{M} and W are given by [30]

$$V_{\mathrm{M}}(y_n) = D(\mathrm{e}^{-ay_n}-1)^2,$$
$$W(y_n, y_{n-1}) = \tfrac{1}{2}S[1+\rho\mathrm{e}^{-b(y_n+u_{n-1})}](y_n-y_{n-1})^2. \tag{3}$$

It is well known that an AT base has two hydrogen bonds while a GC pair has three hydrogen bonds. In this framework, D is the dissociation energy and a stands for a parameter homogeneous to the inverse of a length, which sets the spatial scale of the potential. On the other hand, as soon as one of the two interacting base pairs is open (and not necessarily both simultaneously), the effective coupling constant of $W(y_n, y_{n-1})$ drops from $S(1+\rho)$ to S. This has been shown to bring about a very large qualitative improvement which leads to a sharp transition when realistic parameters are used [29, 30]. In this framework, the parameters used in this work are from [29, 30] and they are $d = 3.4$ Å, $m = 300$ amu, $S = 0.04$ eV Å^{-2}, $D = 0.04$ eV, $a = 4.45$ Å^{-1}, $\rho = 0.5$ and $b = 0.35$ Å^{-1} for the lattice equation (1) and $\chi = 0.6$ eV Å^{-1} for the charge–lattice coupling constant [29].

Charge migration in DNA depends on realistic values of parameters, specifically those related to charge transport and spreading. The values of almost all the parameters are borrowed from experiments, but the value of the transfer integral between nearest pairs remains controversial and therefore raises questions on the validity of the PBH model.

According to experiments, the value of the electron overlap integral V is 0.01 eV [31, 32], which is smaller than the thermal energy $k_{\mathrm{B}}T \sim 0.026$ eV. On the other hand, according to theoretical estimations within the quantum-chemical theory, the value of V lies in the range 0.05–0.3 eV [28, 33, 34]. Because of this discrepancy between theoretical estimations and experimental data, the averaged value widely used for V is 0.1 eV [28, 29]. However, from the values of parameters proposed above, together with the averaged value of V, the adiabatic parameter $\hbar\omega_{\mathrm{ph}}/V$, where $\omega_{\mathrm{ph}} = \sqrt{\frac{1}{m}[2a^2D + 4S(1+\rho)\sin^2(qd/2)]}$ is a characteristic frequency of the lattice phonon (~7 THz), is of the order of 0.05, i.e. well inside the adiabatic regime. This justifies the use of the semiclassical approximation.

The system of units used (amu, Å, eV) defines a time unit (t.u.) equal to 0.010 21 ps. With all these elements, equation (2) can be written as

$$\begin{aligned} m\ddot{y}_n &= S(y_{n+1}+y_{n-1}-2y_n)+\tfrac{1}{2}S[2+b\rho(y_{n+1}-y_n)] \\ &\times (y_{n+1}-y_n)\mathrm{e}^{-b(y_{n+1}+y_n)}-\tfrac{1}{2}S[2-b\rho(y_n-y_{n-1})] \\ &\times (y_n-y_{n-1})\mathrm{e}^{-b(y_n+y_{n-1})}-2aD(\mathrm{e}^{-ay_n}-\mathrm{e}^{-2ay_n}) \\ &-\chi|\psi_n|^2. \end{aligned} \tag{4}$$

Let us recall, in the absence of charge ($\chi = 0$), equation (4) is the generic equation of the Dauxois–Peyrard–Bishop model of DNA dynamics [30]. This model, which is an enhancement of the Peyrard–Bishop model [20], was originally introduced for a description of the structural behavior (specifically the dynamics related to bubble opening of the two strands) of the flexible DNA macromolecule. It has also been widely used in the study of the local melting (or the thermal denaturation) of DNA. It cannot therefore support polaronic solution or describe charge spreading in DNA.

After expanding the terms in exponentials until the third order, the continuum approximation of equations (1) and (4) can be written as

$$\mathrm{i}\frac{\partial\psi}{\partial t}+P_1\frac{\partial^2\psi}{\partial x^2}+Q_1\psi+Q_2y\psi=0 \tag{5a}$$

$$\begin{aligned} &\frac{\partial^2 y}{\partial t^2}-c_0^2\frac{\partial^2 y}{\partial x^2}+\frac{c_1}{2}\frac{\partial^2(y^2)}{\partial x^2}+c_2y\left(\frac{\partial y}{\partial x}\right)^2 \\ &\quad+\omega_g^2(y+\alpha y^2+\gamma y^3)+c_3|\psi|^2=0 \end{aligned} \tag{5b}$$

where

$$\begin{aligned} &P_1=\frac{2Vd^2}{\hbar},\qquad Q_1=\frac{2V}{\hbar},\qquad Q_2=-\frac{\chi}{\hbar}, \\ &c_0^2=\frac{kd^2}{m},\qquad c_1=\frac{bS\rho d^2}{m},\qquad c_2=-\frac{2b^2S\rho d^2}{m} \\ &c_3=\frac{\chi}{m},\qquad \gamma=\beta'+\frac{2b^2S\rho d^2}{\omega_g^2}, \\ &\beta'=\beta+\frac{2b^2S\rho d^2}{\omega_g^2},\qquad \omega_g^2=\frac{2a^2D}{m},\qquad \alpha=-\frac{3a}{2}, \\ &\beta=\frac{7a^2}{6},\qquad k=S(1+\rho). \end{aligned} \tag{6}$$

2.2. Linear stability analysis

In order to perform the linear stability analysis of system (5), we assume that

$$\psi=\psi_0\mathrm{e}^{\mathrm{i}\omega_0 t},\qquad y=y_0 \tag{7}$$

with real constants ω_0, y_0 and complex constant ψ_0. By substituting the above relation into equation (5), we get

$$\omega_0=Q_1+Q_2y_0,\qquad \omega_g^2(y_0+\alpha y_0^2+\beta y_0^3)+c_2|\psi_0|^2=0. \tag{8}$$

By adding a small perturbation in the above equilibrium state, i.e.

$$\psi=(\psi_0+\epsilon\psi_1)\mathrm{e}^{\mathrm{i}Q_2y_0t},\qquad y=y_0+\epsilon y_1, \tag{9}$$

and using it to linearize the mKGS system, with the help of condition (8), we write $\psi_0 = a_1 + \mathrm{i}a_2$, $\psi_1 = u + \mathrm{i}v$ and we separate the real and the imaginary parts as follows:

$$P_1\frac{\partial^2 u}{\partial x^2}-\frac{\partial v}{\partial t}+Q_1u+Q_2a_1y_1=0 \tag{10}$$

$$P_1\frac{\partial^2 v}{\partial x^2}+\frac{\partial u}{\partial t}+Q_1v+Q_2a_2y_1=0 \tag{11}$$

and

$$\begin{aligned} &P_1\frac{\partial^2 y_1}{\partial t^2}+(c_1y_0-c_0^2)\frac{\partial y_1}{\partial x^2}+\omega_g^2(1+2\alpha y_0+2\beta y_0^2)y_1 \\ &\quad+2c_3(a_1u+a_2v)=0. \end{aligned} \tag{12}$$

Furthermore, inserting $u = u_0\mathrm{e}^{\mathrm{i}(Kx-\Omega t)}$ + c.c., $v = v_0\mathrm{e}^{\mathrm{i}(Kx-\Omega t)}$ + c.c. and $y_1 = y_{01}\mathrm{e}^{\mathrm{i}(Kx-\Omega t)}$ + c.c. into equations (10)–(12), where K and Ω are the perturbation wavenumber and the frequency, respectively, which are much smaller than those of the carrier wave, and c.c. stands for the complex conjugate, we arrive at the general nonlinear dispersion relation

$$\Omega^4-P\Omega^2+Q=0 \tag{13}$$

where

$$\begin{aligned} P &= P_1K^4-[2P_1Q_1-(c_1y_0-c_0^2)]K^2+Q_1^2 \\ &\quad+\omega_g^2(1+2\alpha y_0+2\beta y_0^2) \\ Q &= (Q_1-P_1K^2)[P_1(c_1y_0-c_0^2)K^4 \\ &\quad-[P_1\omega_g^2(1+2\alpha y_0+2\beta y_0^2)+Q_1(c_1y_0-c_0^2)]K^2 \\ &\quad+Q_1\omega_g^2(1+2\alpha y_0+2\beta y_0^2)-2c_3Q_2|\psi_0|^2]. \end{aligned} \tag{14}$$

Equation (13) has the solutions

$$\Omega_+^2=\tfrac{1}{2}[P+\sqrt{P^2-4Q}],\qquad \Omega_-^2=\tfrac{1}{2}[P-\sqrt{P^2-4Q}]. \tag{15}$$

For the mKGS model to be modulationally stable for any wavenumber K, $\Omega_\pm^2$ should be positive and this is possible only if the following conditions are simultaneously satisfied:

$$P>0,\qquad Q>0,\qquad \Delta=P^2-4Q>0. \tag{16}$$

In this framework, we have plotted, in figure 1, those three quantities with respect to the wavenumber K and the following features have been observed:

(1) For $P \geqslant 0$, it is obvious that $P = 0$ has two non-zero roots:

$$K_{P\pm}^2=\frac{1}{2P_1}[2P_1Q_1-(c_1y_0-c_0^2)\pm\sqrt{\Delta_P}] \tag{17}$$

where $\Delta_P = [2P_1Q_1-(c_1y_0-c_0^2)]^2-4P_1[Q_1^2+\omega_g^2(1+2\alpha y_0+2\beta y_0^2)]$. Since we are using realistic values of parameters specific to DNA, the parameter V of the PBH model has been found to deeply influence the above condition and the curves for P have been plotted for its different values (see figure 1(a)). For the three cases pointed out, i.e. for $V = 0.05$, 0.10 and 0.15 eV, we have $K_{P-}^2 < 0 < K_{P+}^2$. $P > 0$ is not satisfied for $K^2 < K_{P+}^2$ and increasing V contributes to reducing the region of stability but, as a whole, we have $\Omega_-^2 < 0 < \Omega_+^2$.

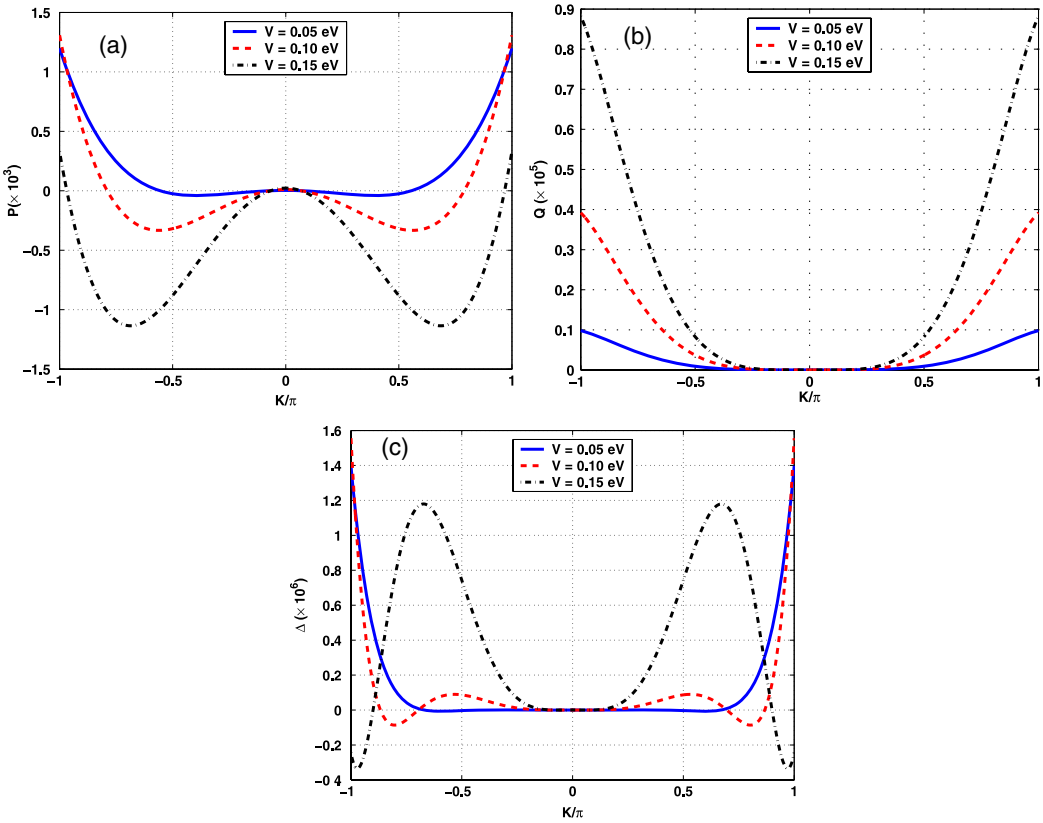

Figure 1. Parameters of the general nonlinear dispersion relation (13) for $m = 300$ amu, $S = 0.04$ eV Å^{-2}, $D = 0.05$ eV, $a = 4.45$ Å^{-1}, $\rho = 0.5$, $b = 0.35$ Å^{-1}, $\chi = 0.6$ eV Å^{-1} and $u_0 = |\psi_0|^2 = 1$.

(2) For $Q \geqslant 0$, it also clear that $Q = 0$ has three non-zero roots:

$$K_{Q1}^2 = \frac{Q_1}{P_1},$$

$$K_{Q\pm}^2 = \frac{P_1\omega_g^2(1 + 2\alpha y_0 + 2\beta y_0^2) + Q_1(c_1 y_0 - c_0^2) \pm \sqrt{\Delta_Q}}{2P_1(c_1 y_0 - c_0^2)} \tag{18}$$

where

$$\Delta_Q = [P_1\omega_g^2(1 + 2\alpha y_0 + 2\beta y_0^2) + Q_1(c_1 y_0 - c_0^2)]^2 - 4P_1(c_1 y_0 - c_0^2)[Q_1^2 + \omega_g^2(1 + 2\alpha y_0 + 2\beta y_0^2) - 2c_3 Q_2|\psi_0|^2].$$

For the set of realistic values chosen, it is clear that $K_{Q-}^2 < 0 < K_{Q+}^2$ as depicted in figure 1(b). As in the previous case, it is clear that increasing V also reduces (but not too much) the region of stability.

(3) The condition $\Delta > 0$ is always satisfied when $Q < 0$. However, it has been shown that $Q > 0$ for $K^2 > K_{Q+}^2$ and, according to the spectrum of behaviors displayed by figure 1(c), the inequality

$$\Delta = d_8 K^8 + d_6 K^6 + d_4 K^4 + d_2 K^2 + d_0 > 0 \tag{19}$$

has many features as depicted in figure 1(c), where

$$d_8 = P_1^2$$

$$d_6 = -2P_1[2P_1 Q_1 - (c_1 y_0 - c_0^2)] + 4P_1^2(c_1 y_0 - c_0^2)$$

$$d_4 = [2P_1 Q_1 - (c_1 y_0 - c_0^2)]^2 + 2P_1 \times [Q_1^2 + \omega_g^2(1 + 2\alpha y_0 + 2\beta y_0^2) - 2c_3 Q_2|\psi_0|^2] + P_1 Q_1(c_1 y_0 - c_0^2) - 4P_1[P_1\omega_g^2(1 + 2\alpha y_0 + 2\beta y_0^2) + Q_1(c_1 y_0 - c_0^2)]$$

$$d_2 = -2[2P_1 Q_1 - (c_1 y_0 - c_0^2)] \times [Q_1^2 + \omega_g^2(1 + 2\alpha y_0 + 2\beta y_0^2) - 2c_3 Q_2|\psi_0|^2] - Q_1[P_1\omega_g^2(1 + 2\alpha y_0 + 2\beta y_0^2) + Q_1(c_1 y_0 - c_0^2)] + 4P_1[Q_1\omega_g^2(1 + 2\alpha y_0 + 2\beta y_0^2) + Q_1(c_1 y_0 - c_0^2)]$$

$$d_0 = [Q_1^2 + \omega_g^2(1 + 2\alpha y_0 + 2\beta y_0^2) - 2c_3 Q_2|\psi_0|^2]^2 + Q_1[Q_1\omega_g^2(1 + 2\alpha y_0 + 2\beta y_0^2) + Q_1(c_1 y_0 - c_0^2)].$$

- For $V = 0.05$ eV, the stability is ensured for $K > 0.75\pi$;
- For $V = 0.1$ eV, the stability region belongs to the intervals $0.25\pi < K < 0.75\pi$ and $K > 0.80\pi$ and finally
- For $V = 0.15$ eV, the stability region is found in the interval $0.2\pi < K < 0.82\pi$.

In summary, the instability is a purely growing mode for $\Delta > 0$ and we have the growth rate instability $\Gamma = \sqrt{-\Omega_-^2}$. On the other hand, if $\Delta < 0$, the solution of (13) is complex. Consequently, the growth rate is determined by the imaginary part $\Gamma = \mathrm{Im}(\Omega_\pm^2) = \pm\sqrt{|\Delta|}/2$.

It is, however, noted that different unstable wavenumber regimes may appear, either partially superimposed or distinct

from each other. Moreover, the tight-binding hopping parameter deeply influences the instability growth rate as shown in figure 2. As a whole, the mKGS system is modulationally unstable when one of the above conditions is violated.

3. Numerical experiment

Linear stability analysis can determine the instability domain in parameter space and predicts qualitatively how the amplitude of a modulation sideband evolves at the onset of the instability. Unfortunately, such an analysis is based on the linearization around the unperturbed carrier wave, which is valid only when the amplitude of the perturbation is small in comparison with that of the carrier wave. Clearly, the linear approximation should fail at large timescales as the amplitude of an unstable sideband grows exponentially. Furthermore, the linear stability analysis neglects the additional combination of waves generated through a wave mixing, which, albeit small at the initial stage, can become significant at large timescales if its wavenumber falls in an instability domain. Linear stability analysis therefore cannot tell us the long time evolution of a modulated wave.

In order to check the validity of our analytical predictions and to explore the formation of intrinsically localized modes in the PBH model, it has been integrated numerically with a fourth-order Runge–Kutta scheme. The accuracy of the calculation is checked by monitoring the conservation of the total energy. Using as the time step $\Delta t = 5\times10^{-3}$ and periodic boundary conditions, the following modulated plane waves are used as initial conditions:

$$\begin{aligned} y_n(t=0) &= y_0[1+0.01\cos(Kn)]\cos(K_0 n),\\ \dot{y}_n(t=0) &= y_0[1+0.01\cos(Kn)]\omega_0\sin(K_0 n)\\ \psi_n(t=0) &= \psi_0(1+0.01\mathrm{e}^{\mathrm{i}Kn})\mathrm{e}^{\mathrm{i}K_0 n} \end{aligned} \qquad (20)$$

where $\omega_0^2 = \omega_g^2 + 4k\sin^2(\frac{K_0}{2})$ is the linear dispersion relation of equation (4), and K and K_0 are the wavenumbers for the perturbation and for the carrier waves, respectively. y_0 and ψ_0 stand for the initial displacement and initial probability for the charge, respectively. For the whole study, we use $y_0 = \psi_0 = 0.02$. Using the realistic values of parameters presented in section 2, wave pattern formation is investigated with an insistence on the impact of the charge-vibrational coupling constant χ.

Beforehand, in figure 3, we see, as expected, the formation of localized structures which have the shape of soliton-like objects. This has been done for $K = \pi/64$ and $K_0 = 3\pi/64$. Two values of χ have been considered: $\chi = 0.4$ eV Å^{-1} (figure 3(a)) and $\chi = 0.8$ eV Å^{-1} (figure 3(b)). If in the first case the patterns are large and distributed with a constant amplitude, the second case shows us how increasing χ influences the distribution and the amplitude of wave patterns. The amplitude is high for the first case and increases gradually for the second. In general, the patterns found here are widely known in the study of MI in DNA dynamics. Dauxois *et al* [30, 35] already suggested that such structures can be precursor

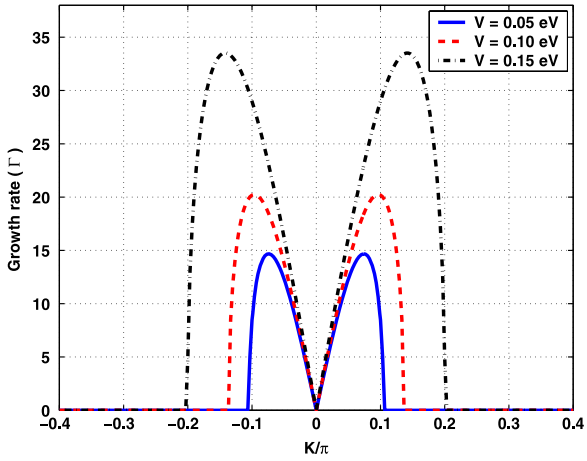

Figure 2. Growth rate versus the wavenumber of the perturbation Q for $m = 300$ amu, $S = 0.04$ eV Å^{-2}, $D = 0.05$ eV, $a = 4.45$ Å^{-1}, $\rho = 0.5$, $b = 0.35$ Å^{-1}, $\chi = 0.6$ eV Å^{-1} and $u_0 = |\psi_0|^2 = 1$.

of the creation of the bubble observed experimentally [36, 37] and in the study of the statistical mechanics of DNA. They also showed that those structures could be used to describe the leading phenomena known as replication and transcription. Since these oscillations of the hydrogen bonds have already been discussed in a submitted work [38], it would be interesting to pay more attention to the features of the charge density. In the meantime, the value of χ determines the decrease in on-site energy in the charged state geometry and has been established theoretically to be in the range of 0.3–1.5 eV Å^{-1} [39]. Its value predominantly depends on the nature of the state geometry and its extension, which can be influenced by the structural parameters of DNA and the solvent environment as well. The charge in DNA can be spread in two directions: in parallel to the propagation pathway (longitudinal direction and perpendicular) transverse direction. The spreading of the charge in the longitudinal direction significantly decreases χ [28]. For the transverse case, a charge can occupy a single purine base that suggests a larger value of χ than does a charge that is partially delocalized over a base pair [39]. With all this in mind, one can obviously see, from figure 4, how increasing χ results in highly localized charge patterns. For $\chi = 0.4$, the patterns are settled but no longer survive (see figure 4(a)). Increasing χ to 0.8 makes the electronic patterns to be more localized but, as seen in figure 4(b), spreads in small radiations after $t = 1000$ t.u. and no longer survive after $t = 1500$ t.u. In the last cases, i.e. $\chi = 1.2$ and 1.5, the electronic patterns survive but in the first case (figure 4(c)) they also spread in small radiations on several sites but, as $\chi = 1.5$, one clearly sees how the patterns are concentrated on specific sites and survive for a long time (see figure 4(d)). Thus, increasing χ results in high localized electronic patterns, which tend to form thin rows on fewer lattices. This result has been suggested by Berashevich *et al* who considered the PBH model in the presence of an electric field [40]. The suggestion that electron and charge transfer/transport in DNA might be biologically important has triggered a series of experimental and theoretical investigations [7, 41]. Processes that probably use charge or

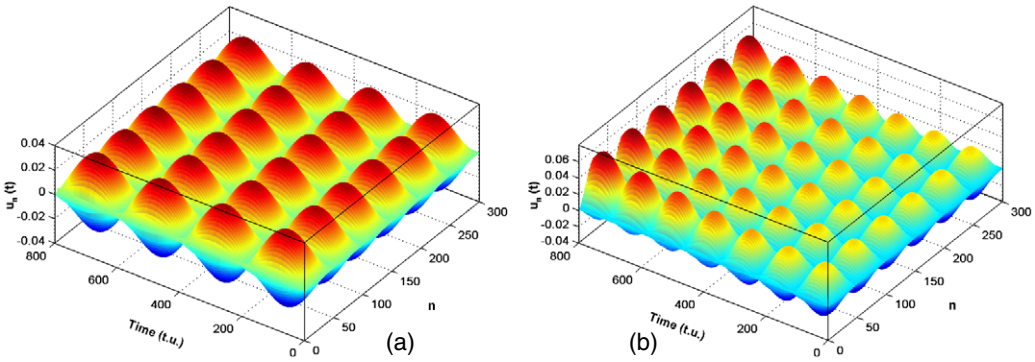

Figure 3. The panels show how the initial plane solution wave breaks into a wave train which has the shape of a soliton-like object in the DNA molecule, as predicted by the analytical predictions, for $m = 300$ amu, $S = 0.04$ eV Å^{-2}, $D = 0.05$ eV, $a = 4.45$ Å^{-1}, $\rho = 0.5$, $b = 0.35$ Å^{-1} and $V = 0.10$ eV and (a) $\chi = 0.4$ eV Å^{-1}; (b) $\chi = 0.8$ eV Å^{-1}.

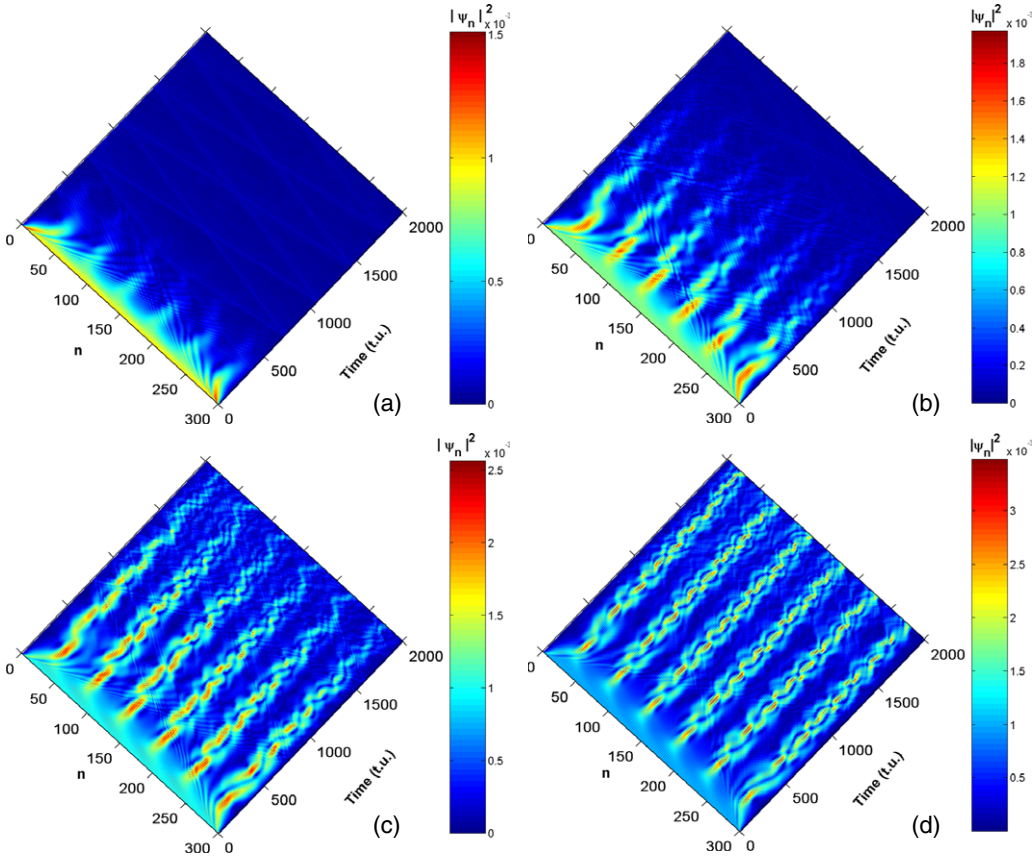

Figure 4. The panels show the space–time evolution of charge instability in the PBH model under the influence of the charge-vibrational coupling constant for $m = 300$ amu, $S = 0.04$ eV Å^{-2}, $D = 0.05$ eV, $a = 4.45$ Å^{-1}, $\rho = 0.5$, $b = 0.35$ Å^{-1} and $V = 0.10$ eV with (a) $\chi = 0.4$ eV Å^{-1}; (b) $\chi = 0.8$ eV Å^{-1}; (c) $\chi = 1.2$ eV Å^{-1}; (d) $\chi = 1.6$ eV Å^{-1}.

electron transfer include the function of DNA damage response enzyme, transcription factors or polymerase co-factors, all of which play important roles in the cell [7, 41].

4. Conclusion

More than 30 years ago, it was suggested that duplex DNA might support electron and charge transport in a manner similar to that of linear chain compounds, namely by tunneling along overlapping π orbitals located on the base pairs. In the meantime, several works have been carried out to substantiate that idea but, unfortunately, the way charges spread in DNA remains not fully understood yet.

Against this background, using the PBH model, we have investigated charge spreading through MI. In this framework, we have shown, in the continuum approximation, through linear stability analysis that MI can also be considered as a

mechanism for charge spreading in the DNA model. The probable regions of MI have been discussed in the same way. Numerical calculations in the original PBH model, i.e. equation (1), confirm the analytical results. Attention has been paid to the impact of the charge-vibrational coupling constant χ and it has been found that increasing the value of χ better enhances charge spreading, in terms of charge pattern, in the model under study.

In our previous works [8], it was shown that the model which describes the stretching of the hydrogen bonds (equation (2) without charge transfer) can respond to any initial condition, soliton or non-soliton. In this framework, under MI, the PBH model exhibits charge transfer in terms of localized structures and solitonic waves. This profoundly probes that MI can be used as a mechanism for charge to be transferred in the DNA duplex. This has been found to be in agreement with recent results [41] and hereby reinforces the efficiency of MI in the bearing of localized structures.

Acknowledgments

CBT acknowledges fruitful discussions with Professor Pierre Ngassam of the Department of Biology and Animal Physiology of the University of Yaoundé I. CBT acknowledges the invitation of the Condensed Matter and Statistical Physics Section (CMSPS) of the Abdus Salam International Centre for Theoretical Physics (ICTP), during which this work was finalized.

References

[1] Eley D D and Spivey D I 1962 *Trans. Faraday Soc.* **58** 411
[2] Snart R S 1968 *Biopolymers* **6** 293
[3] Hoffmann T A and Ladik J 1964 *Adv. Chem. Phys.* **7** 84
[4] Murphy C J *et al* 1993 *Science* **262** 1025
[5] Turro N J and Barton J K 1998 *J. Biol. Inorg. Chem.* **3** 201
[6] Braun E, Eichen Y, Sivan U and Ben-Yoseph G 1998 *Nature* **391** 775
[7] Porath D, Bezryadin A, de Vries S and Dekker C 2000 *Nature* **403** 635
[8] Tabi C B, Mohamadou A and Kofane T C 2008 *J. Phys.: Condens. Matter* **20** 415104
Tabi C B, Mohamadou A and Kofane T C 2008 *J. Comput. Theor. Nanosci.* **5** 647
[9] Bruinsma R, Grüner G, D'Orsogna M R and Rudnick J 2000 *Phys. Rev. Lett.* **85** 4393
[10] Ly D *et al* 1996 *J. Am. Chem. Soc.* **118** 8747
[11] Jortner J 1998 *Proc. Natl Acad. Sci. USA* **95** 12759
[12] Yu Z G and Song X 2001 *Phys. Rev. Lett.* **86** 6018
[13] Hermon Z, Caspi S and Ben-Jacob E 1998 *Europhys. Lett.* **43** 482
[14] Yoo K-H *et al* 2001 *Phys. Rev. Lett.* **87** 198102
[15] Conwell S E and Rakhmanova S V 2000 *Proc. Natl Acad. Sci. USA* **97** 4556
[16] Maniadis P, Kalosakas G, Rasmussen K Ø and Bishop A R 2005 *Phys. Rev.* E **72** 021912
[17] Zhu J-X, Rasmussen K Ø, Balatsky A V and Bishop A R 2007 *J. Phys.: Condens. Matter* **19** 136203
[18] Kalosakas G, Rasmussen K Ø and Bishop A R 2003 *J. Chem. Phys.* **118** 3731
Kalosakas G, Rasmussen K Ø and Bishop A R 2004 *Synth. Met.* **141** 93
[19] Henning D, Starikov E B, Archilla J F R and Palmero F 2004 *J. Biol. Phys.* **30** 227
[20] Peyrard M and Bishop A R 1989 *Phys. Rev. Lett.* **62** 2755
Dauxois T and Peyrard M 1993 *Phys. Rev.* E **47** 3935
[21] Dauxois T, Peyrard M and Bishop A R 1995 *Phys. Rev.* E **51** 4027
[22] Campa A and Giansanti A 1998 *Phys. Rev.* E **58** 3585
[23] Cule D and Hwa T 1997 *Phys. Rev.* E **79** 2375
[24] Wartell R M and Benight A S 1985 *Phys. Rep.* **126** 67
[25] Theordorakopoulos N, Dauxois T and Peyrard M 2000 *Phys. Rev. Lett.* **85** 6
[26] Dauxois T, Theordorakopoulos N and Peyrard M 2002 *J. Stat. Phys.* **107** 869
[27] Komineas S, Kalosakas G and Bishop A R 2002 *Phys. Rev.* E **65** 061905
[28] Berashevich J and Chakraborty T 2007 *Chem. Phys. Lett.* **446** 159
[29] Maniadis P, Kalosakas G, Rasmussen K and Bishop A R 2003 *Phys. Rev.* B **68** 174304
[30] Dauxois T, Peyrard M and Bishop A R 1993 *Phys. Rev.* E **47** R44
[31] Lewis F D, Kalgutkar R J, Wu Y, Liu X, Liu J, Hayes R T, Miller S E and Wasielewski M R 2000 *J. Am. Chem. Soc.* **122** 12346
[32] O'Neill M A, Becker H C, Wan C C, Barton J K and Zewail A H 2003 *Angew. Chem. Int. Edn* **42** 5896
[33] Voityuk A A and Rösch N 2002 *J. Chem. Phys.* **117** 5607
[34] Senthilkumar K, Grozema F C, Guerra C F, Bilkelhaupt F M, Lewis F D, Berlin Y A, Ratner M A and Siebbeles L D A 2005 *J. Am. Chem. Soc.* **127** 14894
[35] Dauxois T, Peyrard M and Willis C R 1992 *Physica* D **57** 267
[36] Saenger W 1984 *Principle of Nucleic Acid Structure* (Berlin: Springer)
[37] Gueron M, Kochoyan M and Leroy J L 1987 *Nature* **328** 89
[38] Tabi C B, Mohamadou A and Kofane T C 2009 submitted
[39] Berashevich J, Apalkov V and Chakraborty T 2008 *J. Phys.: Condens. Matter* **20** 075104
[40] Berashevich J, Bookatz A D and Chakraborty T 2008 *J. Phys.: Condens. Matter* **20** 035207
[41] Berlin Y A, Burin A L and Ratner M A 2000 *J. Phys. Chem.* A **104** 443